Supplemental Materials

Ciliopathy-associated mutations of IFT122 impair ciliary protein trafficking but not ciliogenesis

Mariko Takahara, Yohei Katoh, Kentaro Nakamura, Tomoaki Hirano, Maho Sugawa, Yuta Tsurumi, and Kazuhisa Nakayama

Graduate School of Pharmaceutical Sciences, Kyoto University, Sakyo-ku, Kyoto 606-8501, Japan

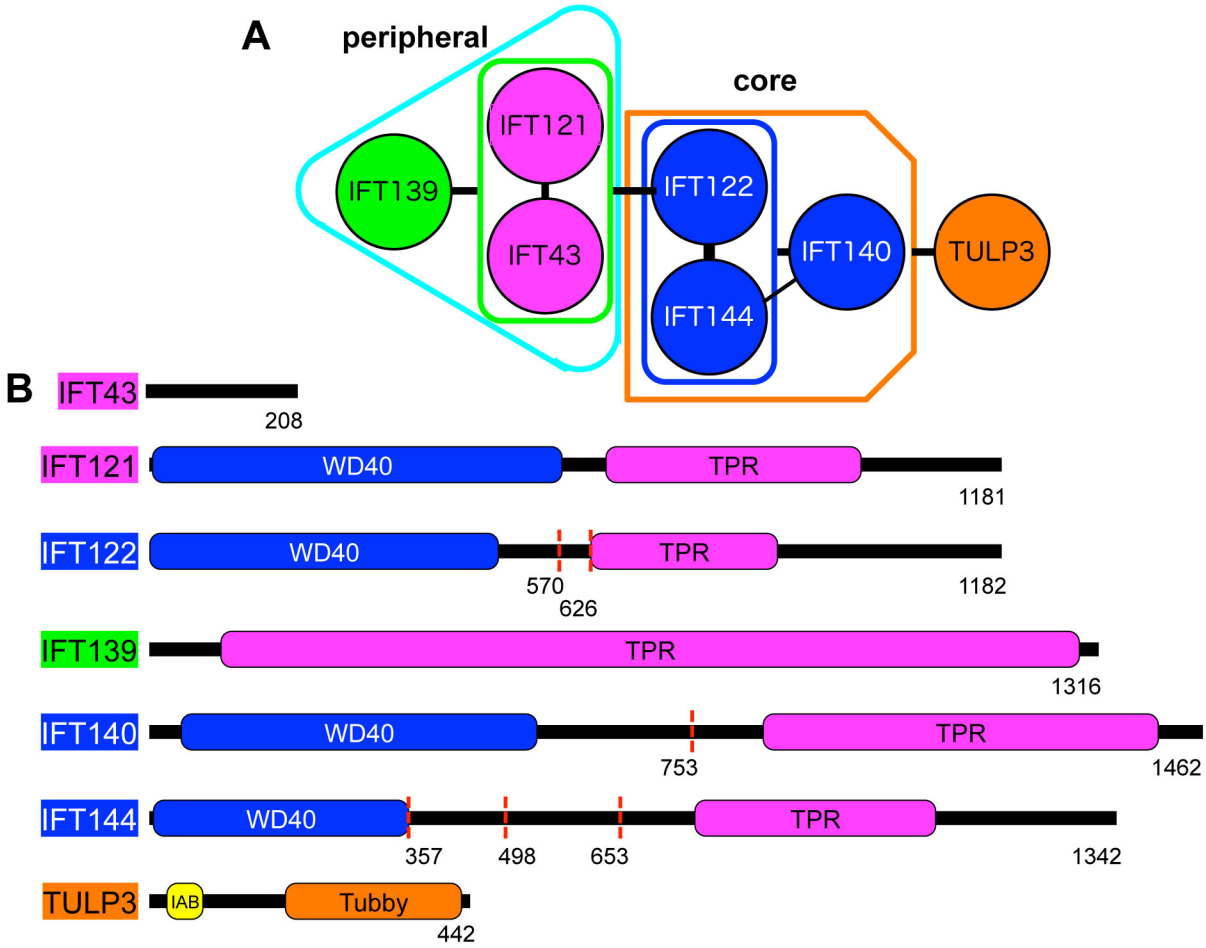

Fig. S1. IFT-A architecture and domain organizations of IFT-A subunits
(A) Architecture of the IFT-A complex predicted from our previous study (Hirano et al., 2017). (B) Domain organizations of the IFT-A subunits. WD40, WD40 repeat domain; TPR, tetratricopeptide repeat domain; IAB, IFT-A–binding motif; Tubby, Tubby-like domain. Red broken lines indicate the positions where the IFT122, IFT140, and IFT144 proteins were divided into the NT and CT regions: IFT122(NT1), aa 1–570; IFT122(NT2), aa 1–626; IFT122(CT), aa 571–1182; IFT140(NT), aa 1–753; IFT140(CT), aa 754–1462; IFT144(NT), aa 1–653; IFT144(CT1), aa 498–1342; and IFT144(CT2), aa 357–1342.

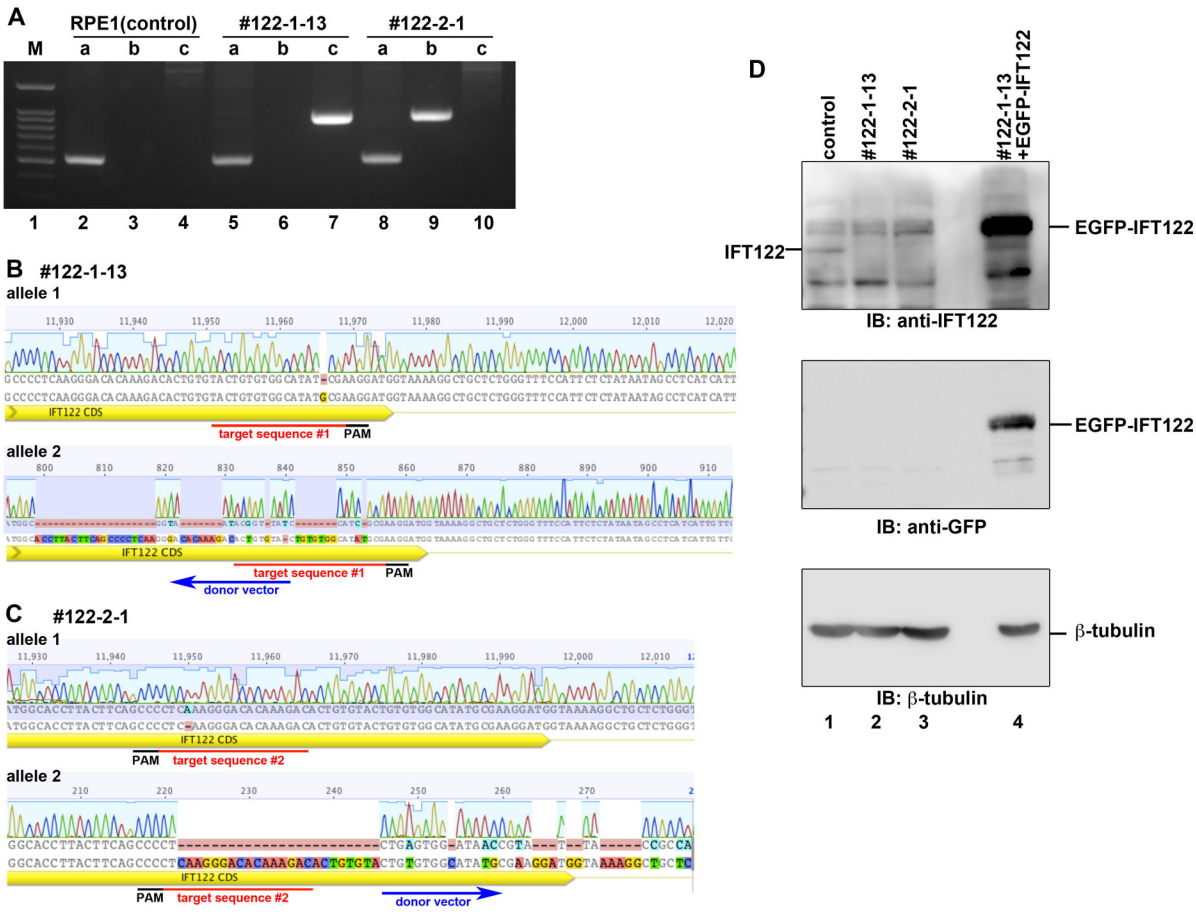

Fig. S2. Genomic PCR and sequencing to confirm donor vector integration in the selected *IFT122*-KO cell lines

(A) Genomic DNA was extracted from control RPE1 cells (lanes 2–4), and from the *IFT122*-KO cell lines (#122-1-13, lanes 5–7; and #122-2-1, lanes 8–10) established using a donor knock-in vector containing target sequences 1 and 2, respectively (see Table S3), which targets the coding region within exon 3 of the human *IFT122* gene. The DNA was subjected to PCR using primer pair a (primers 2 + 3; lanes 2, 5, and 8), pair b (primers 1 + 2; lanes 3, 6, and 9), and pair c (primers 1 + 3; lanes 4, 7, and 10) (see Table S3). Lane 1, a 100-bp ladder marker in which the most intense band is 500 bp. (B and C) Alignments of allele sequences of cell lines #122-1-13 (B) and #122-2-1 (C) determined by direct sequencing of the genomic PCR products with the reference sequence encompassing the coding sequence of exon 3. Red and black lines indicate the target sequences and protospacer adjacent motif (PAM) sequence, respectively. Blue arrows indicate the direction of vector integration. (D) Immunoblotting analysis of the IFT122 protein in control and the *IFT122*-KO cell lines. Lysates from control RPE1 cells (lane 1), #122-1-13 cells (lane 2), and #122-2-1 cells (lane 3) were processed for immunoblotting analysis using antibodies against IFT122 (upper panel), GFP (middle panel), and β-tubulin (lower panel). To confirm the reactivity of the anti-IFT122 antibody, lysates from #122-1-13 cells rescued with EGFP-IFT122(WT) were also subjected to immunoblotting (lane 4). Positions of IFT122, EGFP-IFT122, and β-tubulin are indicated.

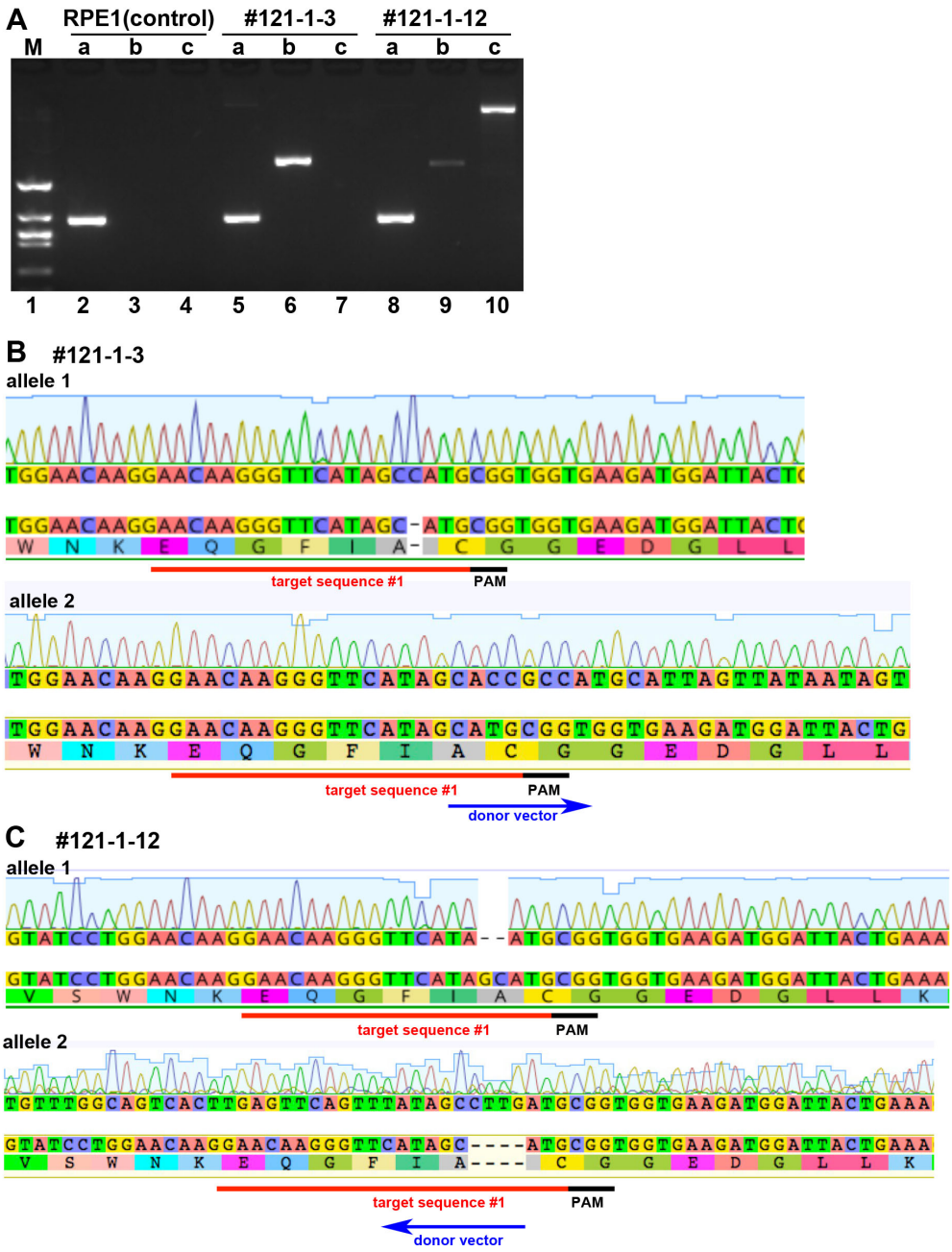

Fig. S3. Genomic PCR and sequencing to confirm donor vector integration in the selected *IFT121*-KO cell lines

(A) Genomic DNA was extracted from control RPE1 cells (lanes 2–4) and from the *IFT121*-KO cell lines (#121-1-3, lanes 5–7; and #121-1-12, lanes 8–10) established using a donor knock-in vector containing a target sequence for the coding region within exon 2 of the human *IFT121* gene (Table S3). The DNA was subjected to PCR using primer pair a (primers 2 + 3; lanes 2, 5, and 8), pair b (primers 1 + 2; lanes 3, 6, and 9), and pair c (primers 1 + 3; lanes 4, 7, and 10) (see Table S3). Lane 1, a DNA marker (pSP64 DNA digested with *DdeI*). (B and C) Alignments of allele sequences of cell lines #121-1-3 (B) and #121-1-12 (C) determined by direct sequencing of genomic PCR products with the reference sequence encompassing the coding sequence of exon 2. Red and black lines indicate the target sequences and PAM sequence, respectively. Blue arrows indicate the direction of vector integration. The #121-1-3 and #121-1-12 cell lines have a forward and reverse integration, respectively, of the donor knock-in vector in one *IFT122* allele (allele 2), and a 1-bp deletion and a 2-bp deletion, respectively, in the other allele (allele 1).

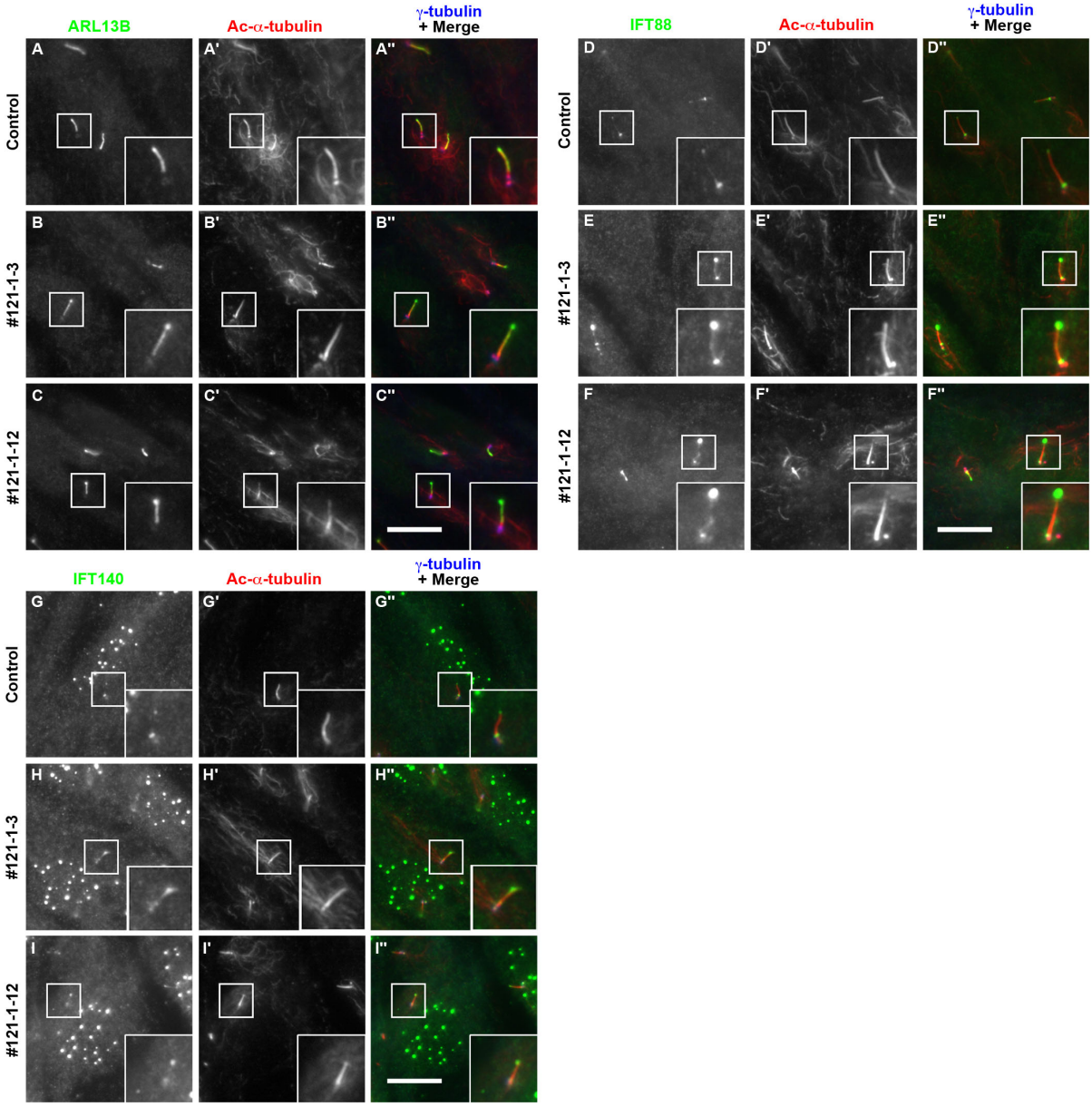

Fig. S4. Accumulation of IFT-A and IFT-B proteins within cilia in *IFT121*-KO cells
Control RPE1 cells (A, D, and G) and the *IFT121*-KO cell lines #121-1-3 (B, E, and H) and #121-1-12 (C, F, and I) were serum-starved for 24 h and triple immunostained for either ARL13B (A–C), IFT88, (D–F) or IFT140 (G–I), together with Ac-α-tubulin (A'–I'), and γ-tubulin (A"–I"). Merged images are shown in A"–I". Insets indicate enlarged images of the boxed regions. Scale bars, 10 µm.

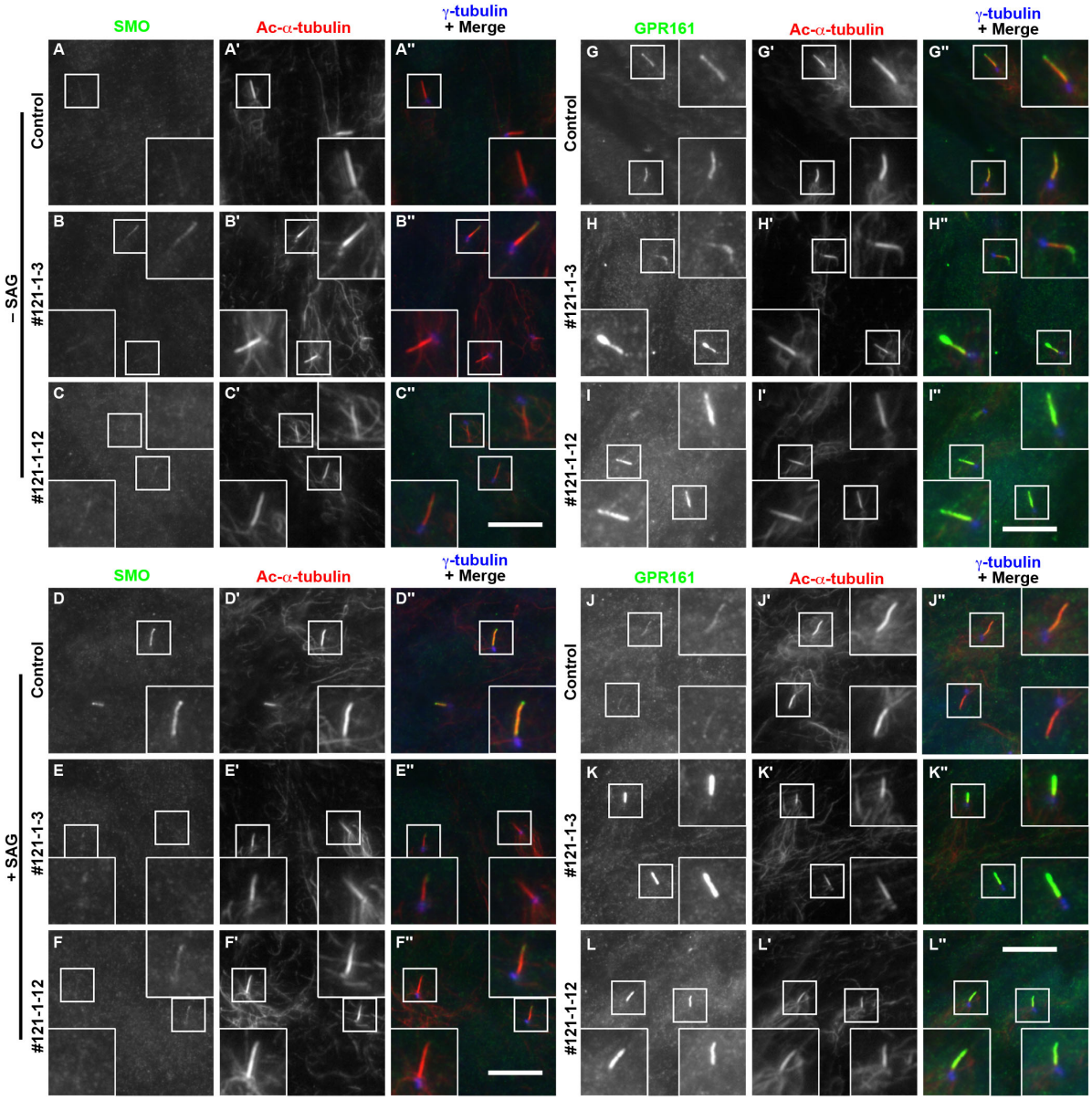

Fig. S5. Defects in retrograde trafficking of GPR161 in response to Hh signaling in *IFT121*-KO cells

Control RPE1 cells (A, D, G, and J), and the *IFT121*-KO cell lines #121-1-3 (B, E, H, and K) and #121-1-12 (C, F, I, and L) were cultured for 24 h under serum-starved conditions to induce ciliogenesis, and for a further 24 h in the absence (–SAG) or presence (+SAG) of 200 nM SAG, and triple immunostained for either SMO (A–F) or GPR161 (G–L), together with Ac-α-tubulin (A'–L'), and γ-tubulin (A"–L"). Merged images are shown in A"–L". Insets indicate enlarged images of the boxed regions. Scale bars, 10 µm.

Table S1. Plasmid vectors used in this study

No	Vectors	Inserts	References
1	pCAG2-EGFP-C	Human IFT122	(Hirano *et al.*, 2017)
2	pCAG2-EGFP-C	Human IFT122 (NT1, 1-570)	This study
3	pCAG2-EGFP-C	Human IFT122 (NT2, 1-626)	This study
4	pCAG2-EGFP-C	Human IFT122(CT, 571-1182)	This study
5	pCAG2-EGFP-C	Human IFT122(W7C)	This study
6	pCAG2-EGFP-C	Human IFT122(S263F)	This study
7	pCAG2-EGFP-C	Human IFT122(G436R)	This study
8	pCAG2-EGFP-C	Human IFT122(V443G)	This study
9	pCAG2-EGFP-C	Human IFT122(G513V)	This study
10	pCAG2-mCherry-C	Human IFT122	(Hirano *et al.*, 2017)
11	pCAG2-mCherry-C	Human IFT122(CT, 571-1182)	This study
12	pRRLsinPPT-EGFP-C	Human IFT122	(Hirano *et al.*, 2017)
13	pRRLsinPPT-EGFP-C	Human IFT122(W7C)	This study
14	pRRLsinPPT-EGFP-C	Human IFT122(G513V)	This study
15	pmCherry-C1	Human IFT43	(Hirano *et al.*, 2017)
16	pCAG2-mCherry-C	Human IFT121	(Hirano *et al.*, 2017)
17	pCAG2-mCherry-C	Human IFT139	(Hirano *et al.*, 2017)
18	pCAG2-EGFP-C	Human IFT140	(Hirano *et al.*, 2017)
19	pCAG2-EGFP-C	Human IFT140(NT, 1-753)	This study
20	pCAG2-EGFP-C	Human IFT140(CT, 754-1462)	This study
21	pCAG2-mCherry-C	Human IFT140	(Hirano *et al.*, 2017)
22	pCAG2-mCherry-C	Human IFT140(NT, 1-753)	This study
23	pCAG2-mCherry-C	Human IFT140(CT, 754-1462)	This study
24	pCAG2-mCherry-C	Human IFT144	(Hirano *et al.*, 2017)
25	pCAG2-mCherry-C	Human IFT144(NT, 1-653)	This study
26	pCAG2-mCherry-C	Human IFT144(CT1, 498-1342)	This study
27	pCAG2-mCherry-C	Human IFT144(CT2, 357-1342)	This study
28	pGEX-6P1	GFP-Nanobody	(Katoh *et al.*, 2015)

Table S2. Antibodies used in this study

Antibodies	Manufacturers	Clones or catalog numbers	Dilution (purpose)
Monoclonal mouse anti-Ac-α-tubulin	Sigma-Aldrich	6-11B-1	1:500 (immunofluorescence)
Monoclonal mouse anti-γ-tubulin	Sigma-Aldrich	GTU88	1:1,000 (immunofluorescence)
Polyclonal rabbit anti-IFT88	Proteintech	13967-1-AP	1:200(immunofluorescence)
Polyclonal rabbit anti-IFT122	Proteintech	19304-1-AP	1:1,000 (immunoblotting)
Polyclonal rabbit anti-IFT140	Proteintech	17460-1-AP	1:100 (immunofluorescence)
Polyclonal rabbit anti-GPR161	Proteintech	13398-1-AP	1:200 (immunofluorescence)
Polyclonal rabbit anti-SMO	Abcam	ab38686	1:100 (immunofluorescence)
Monoclonal mouse anti-GFP	BD Biosciences	JL-8	1:1,000 (immunofluorescence) (immunoblotting)
Polyclonal rabbit anti-RFP	MBL Life Science	PM005	1:1,000 (immunoblotting)
AlexaFluor-conjugated secondary	Molecular Probes	A11034, A21240, A21131 A21147	1:500 (immunofluorescence)
AlexaFluor-conjugated secondary	Molecular Probes	A21429, A21242	1:1,000 (immunofluorescence)
DyLight 649-conjugated secondary	Jackson ImmunoResearch	115-495-209	1:500 (immunofluorescence)
Peroxidase-conjugated secondary	Jackson ImmunoResearch	115-035-166, 111-035-144	1:3,000 (immunoblotting)

Table S3. Oligo DNAs used in this study

No.	Names	Sequences
1	pTagBFP-N-RV	5'-GTTGTCCACGGTGCCCTCCATGTAC-3'
2	IFT122-genome-FW	5'-CCTGGTCACATAGTACATAGACC-3'
3	IFT122-genome-RV	5'-TCTGAAGTAACTCAAGCACCTTG-3'
4	IFT122-gRNA#1-S	5'-CACCGGACTGTGTGGCATATGCGA-3'
5	IFT122-gRNA#1-AS	5'-AAACTCGCATATGCCACACAGTCC-3'
6	IFT122-gRNA#1-donor-AS	5'-TCCATCGCATATGCCACACAGTCC-3'
7	IFT122-gRNA#2-S	5'-CACCGGGTCTTTGTGTCCCTTGAG-3'
8	IFT122-gRNA#2-AS	5'-AAACCTCAAGGGACACAAAGACCC-3'
9	IFT122-gRNA#2-donor-AS	5'-TCCACTCAAGGGACACAAAGACCC-3'
10	IFT121-genome-FW	5'-GAAGAGGGACTGGTGGTATGG-3'
11	IFT121-genome-RV	5'-CATGAGTAGACCGCACTGAAC-3'
12	IFT121-gRNA#1-S	5'-CACCGAACAAGGGTTCATAGCATG-3'
13	IFT121-gRNA#1-AS	5'-AAACCATGCTATGAACCCTTGTTC-3'

Supplementary References

Hirano, T., Katoh, Y., and Nakayama, K. (2017). Intraflagellar transport-A complex mediates ciliary entry and retrograde trafficking of ciliary G protein-coupled receptors. Mol. Biol. Cell *28*, 429-439.

Katoh, Y., Nozaki, S., Hartanto, D., Miyano, R., and Nakayama, K. (2015). Architectures of multisubunit complexes revealed by a visible immunoprecipitation assay using fluorescent fusion proteins. J. Cell Sci. *128*, 2351-2362.